Translational Oncology
www.transonc.com

Volume 11 Number 4 August 2018 pp. 930–940 930

p53 Mediates Vast Gene Expression Changes That Contribute to Poor Chemotherapeutic Response in a Mouse Model of Breast Cancer[1,2]

Crystal Tonnessen-Murray[*,3], Nathan A. Ungerleider[†,3], Sonia G. Rao[*], Amanda R. Wasylishen[‡], Wesley D. Frey[*] and James G. Jackson[*]

[*]Department of Biochemistry and Molecular Biology, Tulane School of Medicine, New Orleans, LA, 70112; [†]Department of Pathology, Tulane School of Medicine, New Orleans, LA, 70112; [‡]Department of Genetics, MD Anderson Cancer Center, 1515 Holcombe Blvd, Houston, TX 77030

Abstract

p53 is a transcription factor that regulates expression of genes involved in cell cycle arrest, senescence, and apoptosis. *TP53* harbors mutations that inactivate its transcriptional activity in roughly 30% of breast cancers, and these tumors are much more likely to undergo a pathological complete response to chemotherapy. Thus, the gene expression program activated by wild-type p53 contributes to a poor response. We used an *in vivo* genetic model system to comprehensively define the p53- and p21-dependent genes and pathways modulated in tumors following doxorubicin treatment. We identified genes differentially expressed in spontaneous mammary tumors harvested from treated MMTV-*Wnt1* mice that respond poorly (*Trp53*+/+) or favorably (*Trp53*-null) and those that lack the critical senescence/arrest p53 target gene *Cdkn1a*. *Trp53* wild-type tumors differentially expressed nearly 10-fold more genes than *Trp53*-null tumors after treatment. Pathway analyses showed that genes involved in cell cycle, senescence, and inflammation were enriched in treated *Trp*53 wild-type tumors; however, no genes/pathways were identified that adequately explain the superior cell death/tumor regression observed in *Trp53*-null tumors. *Cdkn1a*-null tumors that retained arrest capacity (responded poorly) and those that proliferated (responded well) after treatment had remarkably different gene regulation. For instance, *Cdkn1a*-null tumors that arrested upregulated *Cdkn2a* (p16), suggesting an alternative, p21-independent route to arrest. Live animal imaging of longitudinal gene expression of a senescence/inflammation gene reporter in *Trp53*+/+ tumors showed induction during and after chemotherapy treatment, while tumors were arrested, but expression rapidly diminished immediately upon relapse.

Translational Oncology (2018) 11, 930–940

Introduction

The tumor suppressor *TP53* is mutated in ~30% of breast cancers [1]. p53 is a transcription factor that is activated by various cellular stresses, including DNA damage induced by chemotherapy regimens [2]. Following damage to DNA, p53 is phosphorylated and dissociated from its negative regulator, Mdm2, allowing the protein to accumulate and become transcriptionally active [3].

Paradoxically, tumors that harbor a mutation in p53 have a significantly greater probability of achieving a pathological complete response to neoadjuvant chemotherapy [4–8]. Supporting these findings, mouse models of breast cancer have shown that *Trp53* mutant mammary tumors respond better to chemotherapy than *Trp53* wild-type tumors [9–11]. Both mouse mammary tumors [9] and human breast cancers [12] that are wild-type for p53 undergo cell senescence in response to chemotherapy rather than the

Address all correspondence to: James G. Jackson, Tulane School of Medicine, Department of Biochemistry and Molecular Biology, 1430 Tulane Avenue, mail code 8543, New Orleans, LA, 70112. E-mail: jjacks8@tulane.edu

[1] This study was supported by the Department of Defense Breast Cancer Research Program (grant number W81XWH-14-1-0216 to J.G.J.).
[2] Declarations of interest: none.
[3] Contributed equally.
Received 1 May 2018; Revised 3 May 2018; Accepted 3 May 2018

1936-5233/18
https://doi.org/10.1016/j.tranon.2018.05.003

widespread cell death seen in mutant tumors [9]. The greater the extent of residual disease present at the time of surgery following chemotherapy, the less favorable the prognosis for the patient [13]. Thus, because p53 mediated arrest and senescence is a barrier to eradicating tumors and achieving a low residual disease burden, understanding the genes regulated by p53 in this context is of the highest importance.

The fate of a cell with wild-type *TP53*, when exposed to DNA-damaging agents, can be cell cycle arrest, senescence, or apoptosis, which is guided by a transcriptional profile of induced and repressed gene expression [3,14]. Which outcome occurs is decided by variety of factors such as tissue specificity and extent of damage, which are not fully understood [14].

One of the first discovered and arguably one of the most important targets of p53 is the cyclin-dependent kinase inhibitor p21, coded by the gene *Cdkn1a* [15–17]. p21 mediates cell cycle arrest induced by p53 after DNA damage [18–20]. Various cell types lacking p21 fail to arrest after DNA damage, similar to cells lacking p53 [20,21]. Here, we have examined gene expression in MMTV-*Wnt*1 mammary tumors that are *Trp53* wild-type (WT), *Trp53*-null, and *Cdkn1a*-null, following doxorubicin chemotherapy treatment.

Materials and Methods

Mouse Tumors and RNA Sequencing

All tumors used were from MMTV-*Wnt*1 transgenic mice that were $Trp53^{+/+}$, $Trp53^{-/-}$ (null), or $Cdkn1a^{-/-}$ (null) and were previously described [9]. The doxorubicin treatment regimen and harvesting schedule for mice that formed spontaneous tumors have been described [9]. RNA was prepared using Trizol, and RNA sequencing was performed by the MD Anderson Cancer Center Sequencing & Microarray Facility. RNA sequencing libraries were prepared using the TruSeq Stranded Total RNA Library Prep Kit with Ribo-Zero Human/Mouse/Rat Sets A and B (*Trp53*WT) and Illumina TruSeq RNA Library Preparation Kit v2 (*Trp53*null and *Cdkn1a*-null tumors). All samples were aligned to the mm10 genome using the STAR RNA-seq aligner [22]. Gene expression was quantified using RSEM [23], and differential expression was calculated using the EBSeq statistical package with a posterior probability of equal expression (PPEE) < .05 considered statistically significant. To avoid any artifacts introduced by batch effects or library preparations, only intragenotype comparisons were made.

Ingenuity Pathway Analysis (IPA)

Data analysis through IPA IPA®, QIAGEN Redwood City, www.qiagen.com/ingenuity) was performed using the lists of fold changes for significantly expressed protein coding genes after doxorubicin treatment for each genotype. IPA "Upstream Regulators" were determined by overlap between known regulators and targets in the Ingenuity Knowledge Base and the targets expressed in the experimental data (overlap *P* value determined by Fisher's exact test), and the activation z-score, which predicts the direction of regulation. IPA identified "Enriched diseases and biological functions" with a significant *P* value of < .05 as determined by Fisher's exact test.

GSEA Analysis

Gene expression data matrices were constructed for each genotype. As the Kyoto Encyclopedia of Genes and Genomes (KEGG) [24] and REACTOME pathways contained only human protein coding genes, only protein coding genes with an HGNC ID (PMID: 29126148) and a human ortholog were retained for Gene set enrichment analyses (GSEA). Analysis was performed using GSEA version 3.0 (Broad Institute, Cambridge, MA) [25]. One thousand gene set permutations were run for each pathway included in the KEGG pathway database [24] and for pathways related to cell cycle in the REACTOME pathway database [26]. Gene set enrichment was considered significant at an FDR< 0.25 [25].

CIBERSORT Analysis

The CIBERSORT algorithm [27] was used to infer immune cell populations in tumor samples. The training set was constructed using publicly available RNA-seq datasets of purified macrophages, T cells, B cells, and several breast cancer cell lines (accession numbers available upon request). The algorithm was run on a gene expression data matrix of all samples in this study. Each sample was assigned a *P* value following deconvolution. Samples included in our analysis had a deconvolution *P* value <.05.

Selection of True TP53 Targets

Riley et al. identified 129 possible direct targets through searching the literature and narrowing candidates that fulfill three out of four determined criteria, which include RNA and protein levels that are regulated by p53, presence of a p53 response element, reporter expression validation, and successful chromatin immunoprecipitation [28]. Allen et al. employed the small molecule inhibitor of Mdm2, nutlin-3, for 1 hour to specifically activate p53. They then performed global run-on sequencing and identified 198 possible direct targets of p53 [29]. A third study used both chromatin immunoprecipitation sequencing and RNA sequencing to identify 432 genes directly regulated by p53 in mouse cells [30].

Luciferase Reporter Assay In Vivo

The reporter lentiviral vector was made using the backbone CD502A-1 (pCDH-EF1α-MCS cDNA Single Promoter Cloning and Expression Lentivector) from Systems Biosciences and contains 1246 bp 5′ of the transcriptional start site of murine *Cxcl5*, followed by a Luciferase cassette, and another cassette with the EF1 promoter driving mCherry. Lentivirus was prepared in 293 T cells using a standard calcium phosphate transfection protocol. Viral supernatant was collected 48 hours and 72 hours following transfection, filtered (0.45 μm), and used to infect target cells in the presence of polybrene (8 μg/ml). Two MMTV-*Wnt1* tumor orthotopic transplants were established and serially propagated as previously described [9]. Tumors that formed were excised, minced with a razor, filtered through a 50-μm filter, and plated in complete DMEM. One day later, concentrated virus was applied, and 24 hours later, media were changed. Two to 3 days after, cells were trypsinized and ~100,000 mCherry-positive cells were sorted by flow cytometry, washed with PBS, and resuspended in Matrigel and injected into the #4 mammary gland of C57Bl6/j mice. The tumor that formed was verified for mCherry fluorescence and transplanted again into multiple C57Bl6/j mice. When tumors formed, they were measured with calipers as previously described [9], IP injected with 10 μg/g of body weight luciferin, and imaged on an IVIS for fluorescence. Tumor volume was calculated as previously described [9]. Luciferase activity was plotted by average counts/tumor volume and normalized for each tumor transplant.

Results

p53 Dominates the Transcriptional Response to Doxorubicin Treatment in Mammary Tumors

TP53 codes for the transcription factor p53 that transactivates genes following many types of cell stress. In breast cancer, the probability of a pathological complete response to chemotherapy is much lower when *TP53* is wild-type as opposed to mutant [4–8]. This implicates the genes and pathways modulated by p53 as contributors to the persistence of tumor cells as residual disease, promoting eventual relapse. Defining the p53 transcriptional response to chemotherapy is critical for understanding the reason tumors fail to regress and for developing therapies to target persisting cells. RNA sequencing was employed to comprehensively define the *in vivo* transcriptional program activated by p53 in mammary tumors after chemotherapy. Gene expression changes were determined in tumors from mice harvested 24 hours following the fifth consecutive day of doxorubicin treatment [9]. We used MMTV-*Wnt1* transgenic mice that were *Trp53* wild-type (WT), *Trp53-null*, or *Cdkn1a*-null. Tumors that arise in MMTV-*Wnt1* transgenic mice remain wild type for *Trp53* and respond to doxorubicin by undergoing arrest and senescence. If *Trp53* is deleted, mutated, or otherwise null, these tumors instead undergo mitotic catastrophe and cell death, resulting in a clinically superior response [9].

Using a false discovery rate (FDR) < 0.05, we found that *Trp53*WT MMTV-*Wnt1* tumors had 1173 protein-coding genes differentially expressed following treatment (Figure 1, *A left* and *C*). *Cdkn1a*-null tumors had 1603 genes significantly changed (Figure 1, *A right* and *C*).

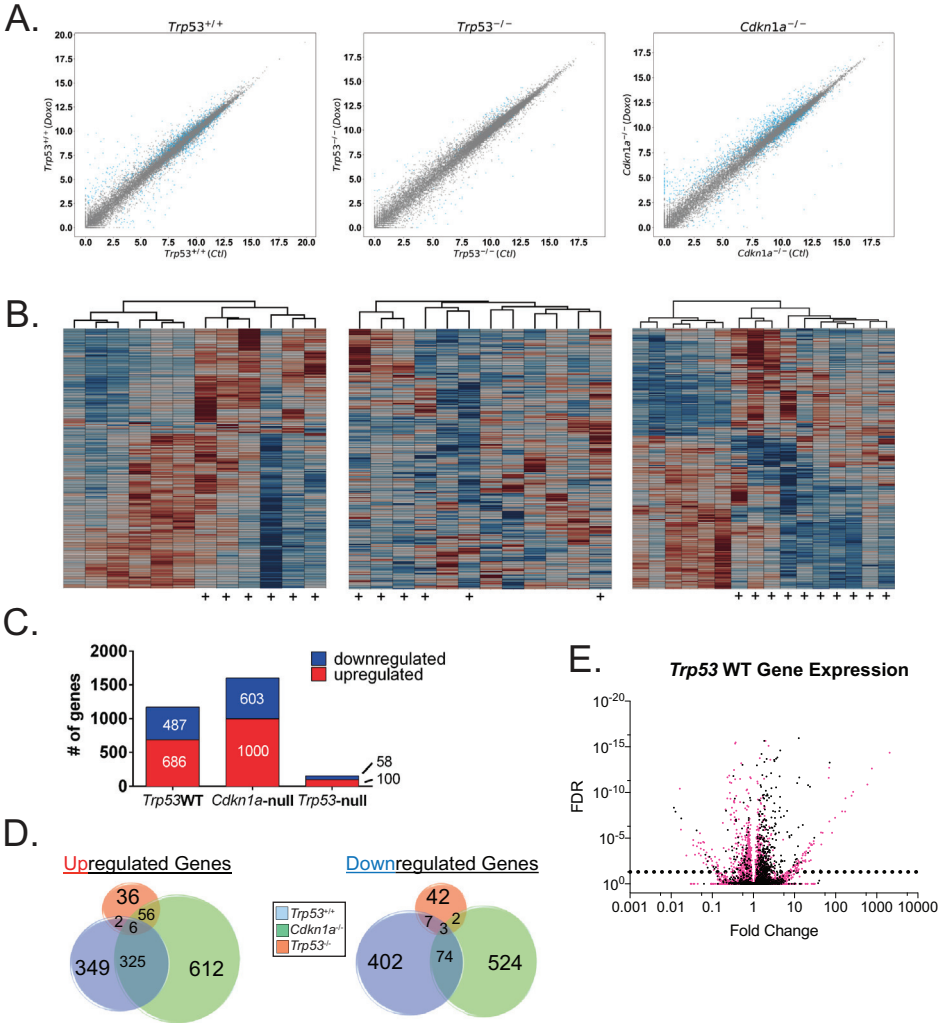

Figure 1. p53 mediates the vast majority of gene expression changes in mammary tumors of mice treated with doxorubicin. MMTV-*Wnt1* transgenic mice with mammary tumors that were *Trp53*$^{+/+}$, *Trp53*$^{-/-}$, or *Cdkn1a*$^{-/-}$ were untreated and harvested (Ctl), or treated with 4 mg/kg doxorubicin IP for 5 consecutive days and then harvested 24 hours following the final treatment (Doxo). (A) After RNA sequencing, scatter plots of differential gene expression in doxorubicin-treated (doxo) versus untreated control (Ctl) were generated for each genotype. Genes significantly changed (PPEE<.05) are represented by a blue point. (B) Heat maps corresponding to genotypes in the scatter plots of (A) were generated for control and doxorubicin-treated (indicated by +) tumors using the union of every differentially expressed gene for each genotype. (C) Bar chart of the total number of significantly regulated protein-coding genes (FDR<0.05) for *Trp53*$^{+/+}$, *Cdkn1a*$^{-/-}$, or *Trp53*$^{-/-}$ cohorts. (D). Venn diagram depicting total numbers of significantly regulated (FDR<0.05) protein-coding genes for each cohort analyzed and the numbers of commonly regulated genes. (E) Volcano plot showing FDR(PPEE) on the *Y*-axis and fold change on the *X*-axis for genes modulated after doxorubicin treatment in *Trp53*$^{+/+}$ tumors. Those genes not significantly regulated in *Cdkn1a*-null tumors are shown in pink.

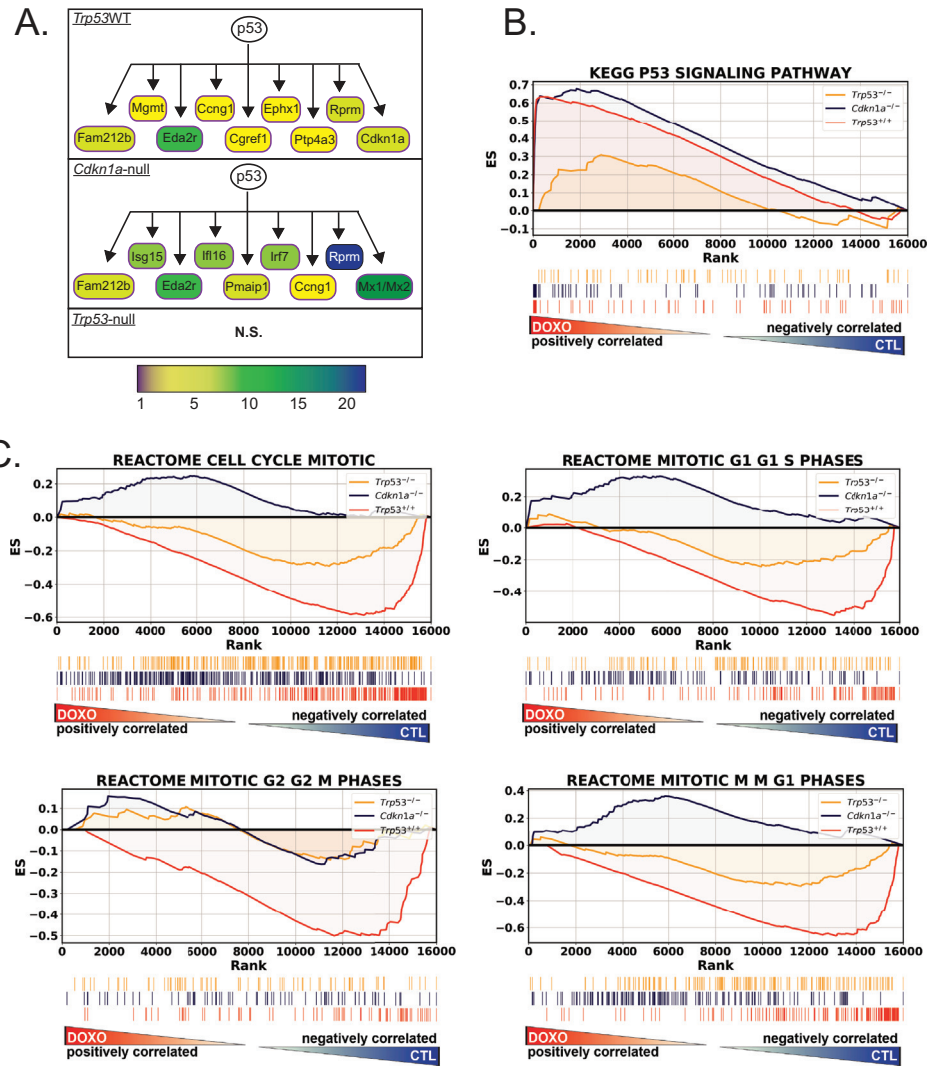

Figure 2. Pathways identified by analysis of doxorubicin-induced gene expression include the p53 pathway and cell cycle. (A) Schematic of top nine upregulated p53 pathway members in each genotype that were identified by IPA as being regulated downstream of p53. Fold change is indicated by color bar. (B) GSEA using KEGG gene lists was performed on RNA-seq data, and running enrichment scores for *Trp53*-null (yellow line), *Cdkn1a*-null (blue line), and *Trp53*WT (orange line) were plotted. Shown under the enrichment score plots are corresponding ranking of genes in the KEGG p53 pathway among ~16,000 genes analyzed. Genes stacked to the left are positively correlated and those to the right negatively correlated with doxorubicin-treated samples. (C) GSEA using the REACTOME cell cycle gene sets for doxorubicin-treated versus untreated tumors for the same genotypes as in B.

In sharp contrast, only 158 genes were significantly changed in *Trp53*-null tumors (Figure 1, *A center* and *C*), despite this genotype responding better to treatment. Heat maps were generated for each genotype that included every differentially expressed gene from each of the three genotypes. Many genes were modulated after doxorubicin treatment in *Trp53*WT and *Cdkn1*a-null tumors (Figure 1*B*), while *Trp53*-null tumors had relatively few genes, and treated tumors did not even cluster entirely together (Figure 1*B, center*). Of note, *Cdkn1a* transcripts were elevated in *Cdkn1a*-null tumors. Aligning reads to the *Cdkn1a* locus showed they were all localized to the 3′ UTR region of the gene and none in the coding region (Supplementary Figure 1), consistent with the knockout strategy used to generate these mice [18].

We next examined overlapping gene expression changes in tumors from the three genotypes. We found that *Trp53*WT and *Cdkn1a*-null tumors shared the regulation of many genes following doxorubicin treatment, while *Trp53*-null had few in common with either tumor genotype (Figure 1*D*). Comparing *Trp53*-null and *Trp53*WT, strikingly, only 18 genes were similarly altered in both, showing that the vast majority of transcriptional changes following doxorubicin treatment are p53 dependent (Figure 1*D*). Interestingly, many genes (760) regulated in *Trp53*WT tumors were no longer regulated in *Cdkn1a*-null tumors (Figure 1*E*), which may reflect a dependence on p21-mediated effects for indirect gene expression changes. Also, while almost half of the genes upregulated in *Trp53*WT tumors were still expressed in *Cdkn1a*-null tumors, only 16% of downregulated genes remain repressed, suggesting that p21 plays a more important role in mediating gene repression by p53 as opposed to induction.

p53 Signaling and Cell Cycle Pathway Analyses in Doxorubicin-Treated Tumors

We next performed gene set enrichment analysis (GSEA) [25] on the 186 gene sets curated by the KEGG [24] as well as IPA to

Table 1. Direct Targets of p53 Identified in Doxorubicin-Treated Mammary Tumors

Riley et al. (129)	Allen et al. (198)	Kenzelmann-Broz et al. (432)	
APAF1	**ABCA1**	*1700007K13Rik*	**Man2b2**
BAX	*AEN*	*Acaa1b*	*Mapkapk3*
BBC3	*APAF1*	**Acox3**	*Mdm2*
BTG2	*ASS1*	*Adrb2*	**Mdm4**
CASP6	*BAX*	*Ak1*	**Mmrn2**
CCNG1	*BBC3*	**Aldh1l1**	*Mybl1*
CDKN1A	*BLOC1S2*	**Alg8**	**Notch1**
CRYZ	*BTG2*	*Bax*	**Npr2**
CTSD	*CCNG1*	*Bbc3*	*Orai2*
CX3CL1	*CDC42BPG*	*Btg2*	**Pdcd6ip**
FAS	*CDKN1A*	*Camk2d*	*Pdk4*
GDF15	*CYFIP2*	*Ccng1*	**Plekhg6**
IRF5	*FAM212B*	*Cd80*	**Pltp**
LIF	*FAS*	*Cdc42bpg*	*Pmaip1*
MDM2	*GDF15*	*Cdkn1a*	*Polk*
MMP2	*GJB5*	*Cgref1*	**Ppm1f**
RPS27L	*ICAM1*	*Cox6b2*	*Pqlc3*
SCN3B	*INPP5D*	*Cpt1c*	**Prrg4**
TAP1	*ISCU*	*Csf1*	*Psrc1*
TNFRSF10B	*KANK3*	*Dcxr*	*Ptp4a3*
TRPM2	*LAPTM5*	*Ddit4l*	*Rap2a*
	LYNX1	**Ddx18**	*Rap2b*
	MDM2	*Def6*	*Rhbdf2*
	ORAI3	*Dennd2c*	*Rprm*
	PHLDA3	**Dut**	*Scn3b*
	POLH	*Eda2r*	*Sema6a*
	RPS27L	*Ei24*	*Sesn2*
	SESN2	*Ephx1*	*Sfmbt1*
	SULF2	*Ercc5*	*Slc19a2*
	TNFRSF10B	*Exoc4*	**Slc4a11**
	TOB1	**Fam53b**	*Sncg*
	TSKU	*Fas*	*Sulf2*
	ZMAT3	*Fbxw9*	*Svop*
		Gas6	*Tbc1d2*
		Gdf15	**Tcirg1**
		Ggta1	*Tmem19*
		Gls2	*Tnfrsf10b*
		Gria3	*Trafd1*
		Gtf3c1	*Trim11*
		H2afx	*Trim7*
		Icam1	*Trp53inp1*
		Kcnj4	**Trp73**
		Klhl26	*Tshr*
		Lif	*Zfp365*

Direct p53 targets identified by previous studies were compared to significantly regulated protein-coding genes in the *Trp53*WT genotype. Table lists genes that were matched, and those genes with an "*" were not found to be regulated in the *Cdkn1a*-null genotype.

determine "upstream regulators" altered after treatment in each of the genotypes. As expected based on the large number of genes regulated (Figure 1*A*), IPA predicted significant activation or inhibition of 94, 204, and 48 molecules as "upstream regulators" of gene expression changes in treated *Trp53*WT, *Cdkn1a*-null, and *Trp53*-null genotypes, respectively (Supplementary Table 1). *Trp53*WT tumors regulated 62 pathways (50 in treated, 12 in control) in the KEGG gene set list (FDR < 0.25) after treatment, and *Cdkn1a*-null tumors regulated 39 (all in treated). *Trp53*-null tumors upregulated only 4 (Supplementary Table 2). Of the 39 pathways upregulated in *Cdkn1a* null tumors, 28 were also upregulated in *Trp53*WT tumors.

Not surprisingly, the "p53 signaling pathway" was a top hit found in both IPA as a predicted "upstream regulator" (Figure 2*A*) and GSEA (Figure 2*B*) analyses for both genotypes with wild-type *Trp53*. GSEA plots depict this enrichment. Many of the genes listed in the p53 pathway KEGG gene set were among the most highly expressed following treatment, resulting in a strong enrichment score in treated samples (Figure 2*B*) and significantly higher leftward peaks in *Trp53*WT and *Cdkna1*-null [0.61, 0.68 enrichment score (ES), respectively, both had FDR < 0.05] than in *Trp53*-null tumors (0.31 ES and nonsignificant FDR = 0.75).

Direct targets of p53 have been identified by multiple studies [28–30]. We used these empirically determined lists to identify the direct p53 target genes regulated in *Trp53*WT tumors after chemotherapy treatment. Many well-known targets were regulated, including *Cdkn1a, Bbc3, Bax*, *Ccng1,* and *Mdm2*. Interestingly, some of these direct p53 targets were not regulated in the *Cdkn1a*-null genotype after treatment (Table 1).

A critical component of the cellular response to DNA damage caused by chemotherapeutics is cell cycle arrest. This arrest is mediated by p53 primarily by transactivating the *Cdkn1a* gene, whose product, p21, is a cyclin-dependent kinase inhibitor [15–17]. We found that gene sets representing all phases of the cell cycle and transitions for G1-S, G2-M, and M-G1 were prominently enriched in the untreated *Trp53* wild-type tumors but were not enriched in either treated or untreated *Trp53*-null tumors (Figure 2*C*). This finding is consistent with the downregulation of cell cycle genes and arrest that occurs in *Trp53* wild-type but not null tumors. Interestingly, *Cdkn1a*-null tumors did not modulate cell cycle genes consistent with either *Trp53* wild-type or null tumors.

Gene Expression Differences in Cdkn1a-Null Tumors That Arrest or Proliferate in Response to Treatment

Next, we separately analyzed the *Cdkn1a*-null tumors according to response phenotype. Unlike in cell culture models [20,21,31], *Trp53* can still mediate a durable G2 arrest in roughly half of treated *Cdkn1a*-null mammary tumors *in vivo* [9]. To investigate this fascinating phenotype, we performed unsupervised hierarchical clustering of differentially expressed genes in all *Cdkn1a*-null tumors after treatment (Figure 3*A*). Untreated tumors and those that continued proliferation into mitotic catastrophe clustered together, while tumors that retained arrest capacity formed two separate clusters (Figure 3*A*). These heat maps show stark differences in gene expression despite the tumors all being the same genotype and receiving the same treatment. In fact, tumors that proliferated in response to treatment had more unique gene expression changes than they had in common with treated tumors that arrested (Figure 3*B*). Examining cell cycle differences in GSEA plots comparing "proliferators" to untreated tumors, we found that treated "proliferators" were actually relatively enriched for cell cycle genes compared to untreated tumors (Figure 3*C*). When treated "arresters" were compared to untreated tumors, relatively more enrichment of cell cycle progression genes was observed in the untreated tumors. The enrichment curve for all *Cdkn1a*-null tumors, i.e., the combination of arresters and proliferators versus control, showed enrichment between the two subphenotypes (Figure 3*C*). We next directly compared gene expression differences in only the treated tumors with either arrester or proliferator phenotypes (without untreated controls). We found that the phenotypes clustered together and many genes were differentially expressed (Figure 3, *D* and *E*). Analysis of the KEGG gene sets showed 43 pathways enriched in arresters and 33 in proliferators (FDR< 0.25; Supplementary Table 3). Analyzing the cell cycle pathways further revealed that proliferators were enriched for most of these genes compared to arresters (Figure 3*F*). Interestingly, *Cdkn2a,* coding for the cyclin-dependent kinase inhibitor p16, was elevated in arresters, suggesting a mechanism for the p53-dependent, p21-independent cell cycle arrest in these tumors (p53 dependent because *Trp53*-null tumors do not arrest). Other genes

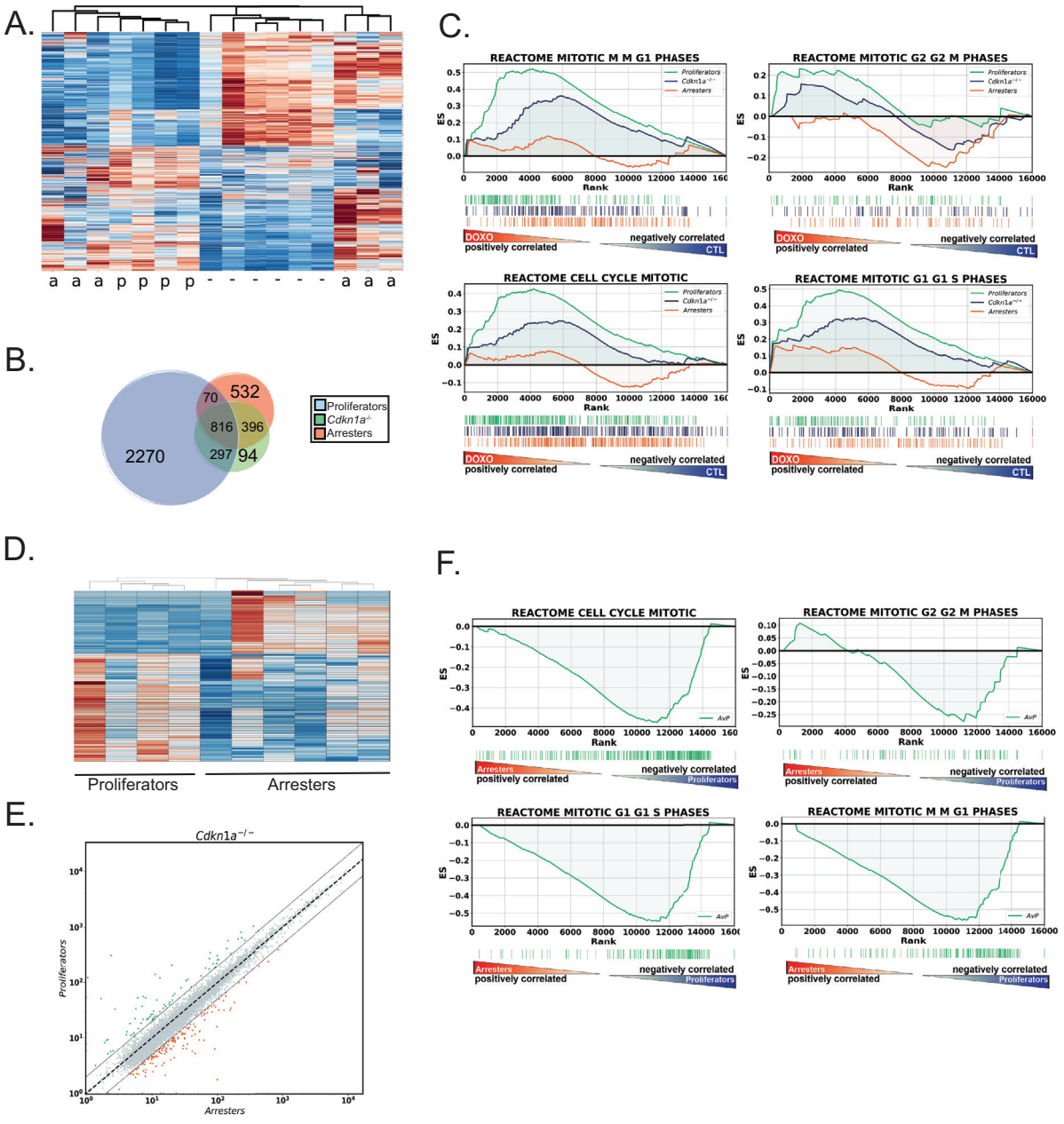

Figure 3. Gene expression patterns differ in *Cdkn1a*-null tumors that respond to doxorubicin with arrest or proliferation. (A) Heat map of untreated *Cdkn1a*-null tumors compared to treated tumors. Those noted as "−" were untreated; those noted as "a" arrested following treatment; and those noted as "p" continued to proliferate after treatment, transiting the cell cycle, consistent with more cell death and a superior response. (B). Venn diagrams showing number of statistically significant (PPEE<.05) gene expression changes after doxorubicin treatment that were shared in the comparisons of untreated tumors to "arresters" and to "proliferators" and in the combination of "arresters" and "proliferators" (*Cdkn1a*$^{-/-}$). (C) GSEA using REACTOME cell cycle gene sets for gene expression comparisons of untreated to "arresters" and untreated to "proliferators." (D) Heat map of gene expression in treated *Cdkn1a*-null tumors that arrested and treated tumors that proliferated. (E) Scatter plot of differentially expressed genes in doxorubicin-treated *Cdkn1a*-null tumors that arrested (*X*-axis) and proliferated (*Y*-axis). (F) GSEA for REACTOME cell cycle gene sets using gene expression comparison of arresters to proliferators as made in D and E.

elevated in arresters include *Wee1* and *Rbl2*. Genes elevated in proliferators include mediators of cell cycle progression *E2f1, Cdk4, Cdk1, Ccnd2, Ccnb2*, and *Cdc25a*. DNA replication pathway and genes were elevated in proliferators, including *Cdt1, Rpa1*, polymerases, and chromosome maintenance genes.

Following chemotherapy treatment, *Trp53*-null tumors and those *Cdkn1a*-null tumors that respond with continued proliferation will undergo cell death and significant tumor regression [9]. Patients with *TP53* mutant tumors are also much more likely to undergo a complete pathological response to chemotherapy [4–8]. Interestingly, apoptosis-related gene pathways in the mammary tumors that undergo cell death and regression were not enriched compared to those that arrest and regress minimally (Supplementary Figure 2). These data suggest that an apoptosis-related transcriptional program is insufficient to induce cell death in treated tumors unless cell cycle arrest is absent. Alternatively, nontranscriptional regulation of apoptotic proteins could mediate the extensive cell death but is not detected in our study.

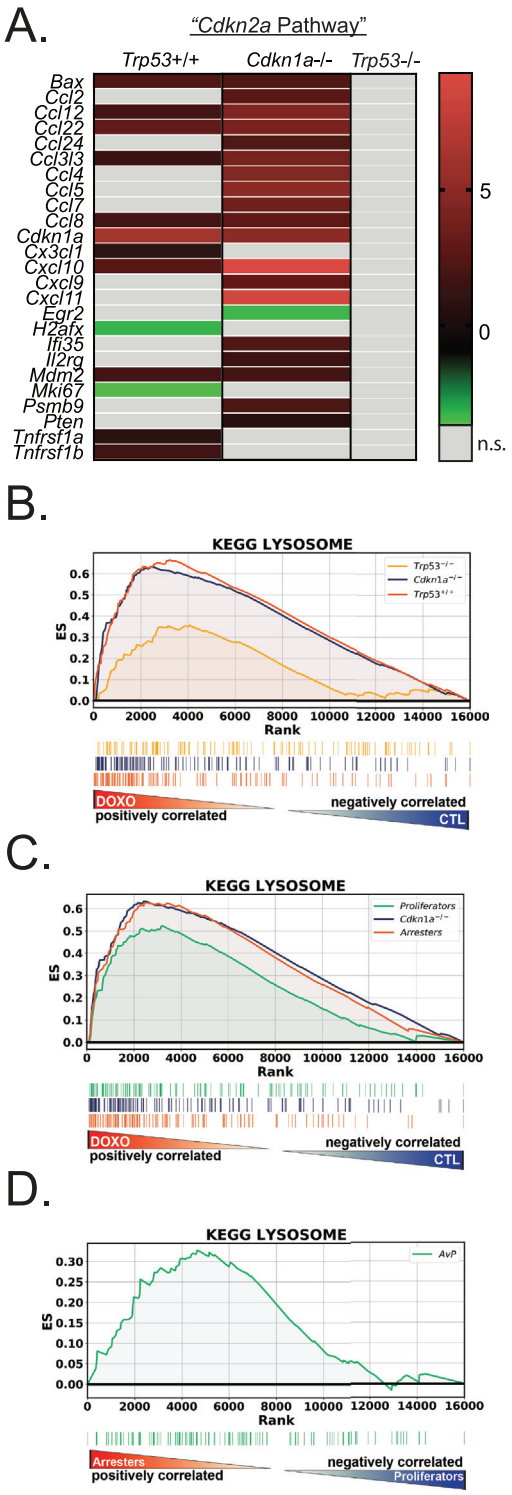

Figure 4. Senescence phenotype is induced by doxorubicin treatment in *Trp53* wild-type tumors. (A) Heat map of the genes and their expression (color bar ranges from -2.2 to 8.3) from each genotype whose products were identified by IPA for upstream regulation by *Cdkn2a*. (B) GSEA using the KEGG Lysosome gene set was performed on doxorubicin-treated versus untreated tumors for *Trp53*WT, *Trp53*-null, and *Cdkn1a*-null genotypes. (C) GSEA using KEGG Lysosome gene set for gene expression comparisons of *Cdkn1a*-null untreated tumors to "arresters" and untreated to "proliferators." (D) GSEA for KEGG Lysosome gene set using gene expression comparison between treated *Cdkn1a* null tumors that arrested compared to treated tumors that proliferated.

Senescence and SASP Genes Are Upregulated in Trp53 Wild-Type Tumors after Treatment

While *Cdkn2a* was not induced by doxorubicin, IPA identified "*Cdkn2a*" as an upstream regulator of the gene expression changes in treated tumors with wild-type *Trp53*. This was due to regulation of gene expression that IPA associates with *Cdkn2a* activity (Figure 4*A*, Supplementary Table 1). *Cdkn2a* codes for the cyclin-dependent kinase inhibitor p16 [32], and due to the prominent role of p16 as a marker and mediator of senescence [33,34], we examined enriched gene sets for other senescence-related pathways. Indeed, other KEGG gene sets regulated in treated tumors with *Trp53* wild-type (including *Cdkn1a*-null) included those related to lysosome, inflammation, and immune responses. Expression of genes involved in lysosome biogenesis is consistent with treated tumors having senescence-associated beta galactosidase (SAβGal) [35,36]. The gene set for "Lysosome" was enriched in treated tumors that had wild-type *Trp53* but not tumors null for *Trp53* (Figure 4*B*). The lysosome pathway was also enriched in the *Cdkn1a*-null tumors that arrested after treatment (Figure 4, *C* and *D*).

In all of the genotypes, enrichment of inflammatory genes and pathways was identified by all of the analyses we performed, which is consistent with these tumors acquiring the senescence-associated secretory phenotype (SASP) [37,38]. Analysis using the PANTHER pathway database [39,40] identified "Inflammation mediated by chemokine and cytokine signaling" as the top hit with greatest number of genes matched for the treated *Trp53* wild-type tumors (Supplementary Table 4). IPA for diseases and biological functions identified "inflammatory response functional category" (Supplementary Table 5) as highly significant and "active" in *Trp53* wild-type tumors but not *Trp53* null. In our GSEA KEGG analysis, 24 out of 50 significantly regulated pathways in *Trp53*WT tumors were immune/inflammation related (Supplementary Table 2). Of the four pathways enriched in *Trp53* null tumors, 3 were immune/inflammation related. These data are consistent with a SASP induced by DNA damage. While SASP is p53 independent [41,42], the fewer immune-related pathways and thus diminished SASP in *Trp53*-null tumors likely represent a transient expression of these genes, as those cells with DNA damage adequate to induce SASP probably end up dying. Senescent *Trp53*WT tumors arrest, survive, persist, and generate SASP over days following treatment and thus generate stronger enrichment of these pathways. Figure 5 shows gene enrichment of the KEGG Jak/Stat signaling and cytokine-cytokine receptor pathways in all three genotypes in the treated tumors. Other immune/SASP-related pathways showed similar patterns, but enrichment of the pathway for treated *Trp53*null tumors did not reach significance (not shown).

Because activation of immune/inflammation pathways was so prominent, we analyzed immune infiltration by CIBERSORT [27]. Our results indicate minimal recruitment of immune cells into the tumor following treatment, as only macrophages were significantly increased (Figure 5*B*). This lack of immune cell presence and tumor clearance at this time point is consistent with previous findings that *Trp53*WT tumors regress minimally and relapse quickly in response to treatment [9]. These data suggest that the superior regression observed in *Trp53*-null tumors is not due to immune clearance.

We next examined SASP-related pathways in the various *Cdkn1a*-null tumor response phenotypes. We found that when both were compared to untreated tumors, arresters had a greater enrichment score for SASP pathways (Figure 5*C*). The finding that arrestors persist and produce more cytokines than proliferators that die by

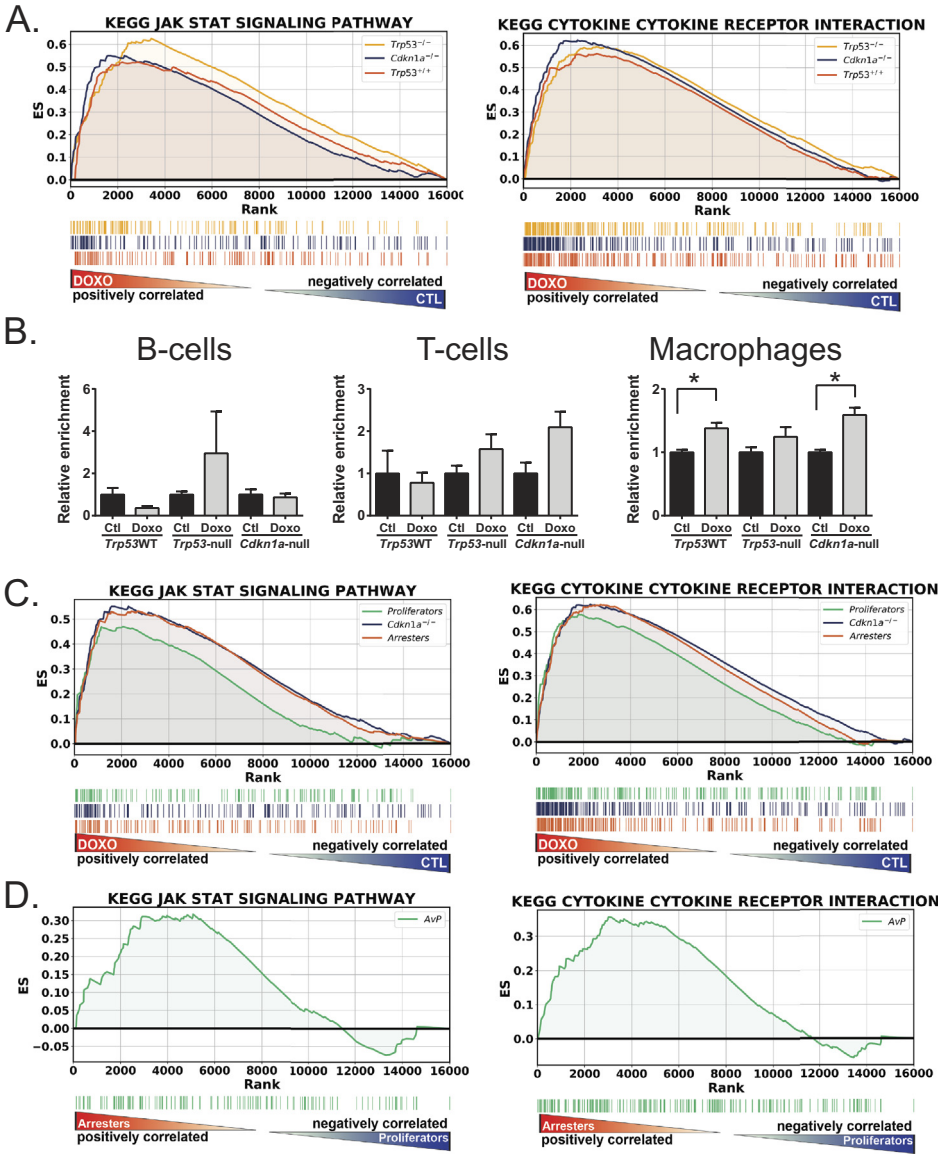

Figure 5. Inflammatory genes are expressed in doxorubicin-treated mammary tumors. (A) GSEA using the KEGG Jak Stat and KEGG cytokine-cytokine receptor interaction gene sets was performed on doxorubicin-treated versus untreated tumors for *Trp53*WT, *Trp53*-null, and *Cdkn1a*-null genotypes. (B) CIBERSORT analysis was performed on gene expression data from *Trp53*WT, *Trp53*-null, and *Cdkn1a*-null genotypes, and relative enrichment of signatures for B cells, T cells, and macrophages was determined and graphed. *t* tests were performed for control (ctl) and doxorubicin-treated (doxo) tumors, * represents $P < .05$. (C) GSEA using KEGG Jak Stat and KEGG cytokine-cytokine receptor interaction gene sets was performed on doxorubicin-treated versus control tumors for gene expression comparisons of *Cdkn1a*-null untreated tumors to "arresters" and untreated to "proliferators." (D) GSEA for KEGG Jak Stat and KEGG cytokine-cytokine gene sets was performed on treated *Cdkn1a*-null tumors that arrested compared to treated tumors that proliferated.

mitotic catastrophe is better illustrated by directly comparing arresters to proliferators (Figure 5*D*).

Longitudinal Expression of Senescence Genes

One limitation of our analysis thus far is the utilization of a single time point, 24 hours post final treatment. Senescence is induced over time, and *Trp*53 wild-type tumors in the MMTV-*Wnt1* model system respond to chemotherapy for a period, usually 1 to 3 weeks, before they eventually relapse [9]. Thus, after observing the expression of senescence and SASP genes 24 hours after the final doxorubicin injection, we next used *in vivo* imaging to quantitate activity of the promoter of a senescence SASP gene starting before treatment, during treatment and response, and then after relapse.

We found that in both independent transplant lines examined, the *Cxcl5* promoter was relatively inactive in untreated tumors as they grew, expressing stably in one transplant (transplant 2) and diminishing somewhat in another (transplant 1, Figure 6*A*). Likewise, when tumors were imaged before treatment, *Cxcl5* promoter activity levels were relatively low (Figure 6*B*). Following treatment, however, promoter activity of the SASP gene spiked just after the final doxorubicin injection. Interestingly, as soon as tumors began to relapse, *Cxcl5* promoter activity rapidly decreased to baseline levels and remained low until the end of the experiment. Thus, promoter

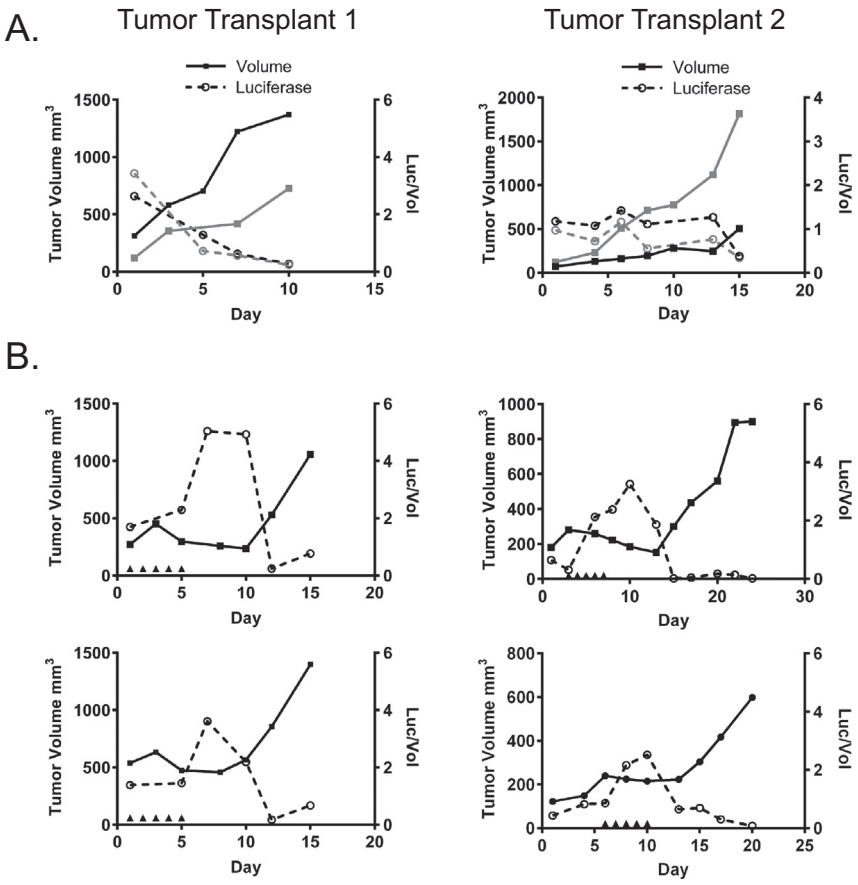

Figure 6. Longitudinal expression of SASP senescence gene *Cxcl5* over the course of treatment and relapse. C57Bl6/j mice were orthotopically transplanted with two different *Trp53*$^{+/+}$, MMTV-*Wnt1* tumors that express luciferase under the control of the *Cxcl5* promoter region. Tumor volume was determined (solid lines, solid squares), and mice were imaged for luciferase expression (dashed line, open circles) regularly. Mice were left untreated (A) or were treated with five consecutive IP injections of 4 mg/kg doxorubicin (B) as indicated by arrowheads on the *X*-axis. Data are expressed graphically with tumor volume indicated by solid lines on the left *Y*-axis and luciferase activity normalized to tumor volume indicated by dashed lines on the right *Y*-axis.

activity of the SASP gene *Cxcl5* is highly transient in the tumor, turning on during or just following treatment and then decreasing rapidly as tumor volume begins to increase again.

Discussion

Increasingly more data from more tumor types show that *TP53* wild-type tumors respond poorly to treatment compared to *TP53* mutant tumors, including tumors of the ovary, lung, mesothelium, colon, bladder, and rectum [43–51]. p53 exerts its effects by regulating transcription of targets involved in cell cycle arrest, senescence, apoptosis, and metabolism, among other functions [2]. When p53 is mutant and unable to activate or repress these genes following chemotherapy, cells fail to arrest and therapeutic response is more robust [9]. In this study, we have used a genetic model system to comprehensively define p53-dependent genes and pathways modulated in tumors following doxorubicin treatment *in vivo*.

Interestingly, we were unable to identify any apoptotic pathway genes that would explain the superior tumor regression in the *Trp53*-null tumors. Gene set enrichment for pathways associated with "apoptosis," "necrosis," "survival," "DNA fragmentation," and "regulation of apoptosis" was not noted to be different for tumors that undergo massive cell death (*Trp53*-null, *Cdkn1a*-null proliferators) compared to tumors that arrest and resist apoptosis (*Trp53*WT tumors, *Cdkn1a*-null arresters). Many apoptotic genes were upregulated in the treated *Trp53*WT tumors, but these tumors undergo only minimal cell death or regression. In clinical studies, *TP53* wild-type tumors also exhibit inferior tumor regression. Based on these data, the most likely scenario seems to be that the *Trp53*-null and *Cdkn1a*-proliferator tumor cells die by transcription-independent means that include apoptosis, necrosis, and mitotic catastrophe.

In tissue culture cells, when *Cdkn1a* is knocked out or down, cells fail to arrest and continue into mitosis and eventually die, similar to p53 null cells [20,21,31]. While p21 is critical for cell cycle arrest in tissue culture, the knockout mouse has a surprisingly mild phenotype [18,52]. In the mammary tumor model, remarkably, tumors with *Cdkn1a* null genotypes could respond with arrest, or bypass arrest and enter mitosis, resulting in a superior response [9]. Among the 10 doxorubicin-treated *Cdkn1a* null tumors in this study, 6 responded with arrest, and 4 failed to arrest as evidenced by the presence of mitotic figures [9]. We analyzed these two cohorts and observed first that these two phenotypes cluster separately. Performing GSEA, we found among the top hits were "Cell Cycle" which showed that *Cdkn2a* (p16) was elevated in the tumors undergoing arrest. In fact, GSEA showed many differences (Supplementary Table 3). Presence of more cytokines in the tumors undergoing arrest is

consistent with observations in p53 null tumors: when enough DNA damage occurs to activate the SASP, tumor cells that are p53 or p21 null (with "proliferator" response phenotype) fail to arrest and likely die, and thus do not persist and produce cytokines.

Our data also suggest that as a tumor relapses, expression of SASP factors such as *Cxcl5* diminishes rapidly. It is not clear if this represents overtaking of the tumor by proliferating nonsenescent cells or, alternatively, if once-senescent cells lose expression of SASP factors and possibly reenter proliferation.

Gene expression analysis in our *in vivo* genetic model system revealed genes and pathways that are differentially activated or repressed in tumors of distinct genotypes and phenotypes, thus defining the programs that result in a poor clinical response. As more studies demonstrate more varieties of *TP53* wild-type tumors that respond poorly to chemotherapy, identifying the genes regulated by p53 will be critical to overcoming this poor response.

Supplementary data to this article can be found online at https://doi.org/10.1016/j.tranon.2018.05.003.

Acknowledgements

The authors wish to acknowledge Melody C. Baddoo and the Tulane Cancer Center Cancer Crusaders Next Generation Sequence Analysis Core supported by the NIH Award Number P01CA214091, and the MD Anderson Cancer Center Sequencing & Microarray Facility, funded by the Core grant CA016672 (SMF). The content is solely the responsibility of the authors and does not necessarily represent the official views of the National Institutes of Health.

References

[1] TCGA-Network (2012). Comprehensive molecular portraits of human breast tumours. *Nature* **490**, 61–70.

[2] Tonnessen-Murray C, Lozano G, and Jackson JG (2016). In: Lozano G, Levine AJ, editors. The p53 Protein: From Cell Regulation to Cancer. Cold Spring Harbor, NY: Cold Spring Harbor Laboratory Press; 2016. p. 173–186.

[3] Kastenhuber ER and Lowe SW (2017). Putting p53 in context. *Cell* **170**, 1062–1078.

[4] Esserman LJ, Berry DA, Cheang MC, Yau C, Perou CM, Carey L, DeMichele A, Gray JW, Conway-Dorsey K, and Lenburg ME, et al (2012). Chemotherapy response and recurrence-free survival in neoadjuvant breast cancer depends on biomarker profiles: results from the I-SPY 1 TRIAL (CALGB 150007/150012; ACRIN 6657). *Breast Cancer Res Treat* **132**, 1049–1062.

[5] Wang Y, Xu Y, Chen J, Ouyang T, Li J, Wang T, Fan Z, Fan T, Lin B, and Xie Y (2015). TP53 mutations are associated with higher rates of pathologic complete response to anthracycline/cyclophosphamide-based neoadjuvant chemotherapy in operable primary breast cancer. *Int J Cancer* **138**, 489–496.

[6] Chen MB, Zhu YQ, Xu JY, Wang LQ, Liu CY, Ji ZY, and Lu PH (2012). Value of TP53 status for predicting response to neoadjuvant chemotherapy in breast cancer: a meta-analysis. *PLoS One* **7**e39655.

[7] Bertheau P, Turpin E, Rickman DS, Espie M, de Reynies A, Feugeas JP, Plassa LF, Soliman H, Varna M, and de Roquancourt A, et al (2007). Exquisite sensitivity of TP53 mutant and basal breast cancers to a dose-dense epirubicin-cyclophosphamide regimen. *PLoS Med* **4**e90.

[8] Bertheau P, Plassa F, Espie M, Turpin E, de Roquancourt A, Marty M, Lerebours F, Beuzard Y, Janin A, and de The H (2002). Effect of mutated TP53 on response of advanced breast cancers to high-dose chemotherapy. *Lancet* **360**, 852–854.

[9] Jackson JG, Pant V, Li Q, Chang LL, Quintas-Cardama A, Garza D, Tavana O, Yang P, Manshouri T, and Li Y, et al (2012). p53-mediated senescence impairs the apoptotic response to chemotherapy and clinical outcome in breast cancer. *Cancer Cell* **21**, 793–806.

[10] Ma CX, Cai S, Li S, Ryan CE, Guo Z, Schaiff WT, Lin L, Hoog J, Goiffon RJ, and Prat A, et al (2012). Targeting Chk1 in p53-deficient triple-negative breast cancer is therapeutically beneficial in human-in-mouse tumor models. *J Clin Invest* **122**, 1541–1552.

[11] Varna M, Lehmann-Che J, Turpin E, Marangoni E, El-Bouchtaoui M, Jeanne M, Grigoriu C, Ratajczak P, Leboeuf C, and Plassa LF, et al (2009). p53 dependent cell-cycle arrest triggered by chemotherapy in xenografted breast tumors. *Int J Cancer* **124**, 991–997.

[12] te Poele RH, Okorokov AL, Jardine L, Cummings J, and Joel SP (2002). DNA damage is able to induce senescence in tumor cells in vitro and in vivo. *Cancer Res* **62**, 1876–1883.

[13] Symmans WF, Peintinger F, Hatzis C, Rajan R, Kuerer H, Valero V, Assad L, Poniecka A, Hennessy B, and Green M, et al (2007). Measurement of residual breast cancer burden to predict survival after neoadjuvant chemotherapy. *J Clin Oncol* **25**, 4414–4422.

[14] Jackson JG, Post SM, and Lozano G (2011). Regulation of tissue- and stimulus-specific cell fate decisions by p53 in vivo. *J Pathol* **223**, 127–136.

[15] el-Deiry WS, Tokino T, Velculescu VE, Levy DB, Parsons R, Trent JM, Lin D, Mercer WE, Kinzler KW, and Vogelstein B (1993). WAF1, a potential mediator of p53 tumor suppression. *Cell* **75**, 817–825.

[16] Xiong Y, Hannon GJ, Zhang H, Casso D, Kobayashi R, and Beach D (1993). p21 is a universal inhibitor of cyclin kinases. *Nature* **366**, 701–704.

[17] Noda A, Ning Y, Venable SF, Pereira-Smith OM, and Smith JR (1994). Cloning of senescent cell-derived inhibitors of DNA synthesis using an expression screen. *Exp Cell Res* **211**, 90–98.

[18] Brugarolas J, Chandrasekaran C, Gordon JI, Beach D, Jacks T, and Hannon GJ (1995). Radiation-induced cell cycle arrest compromised by p21 deficiency. *Nature* **377**, 552–557.

[19] Deng C, Zhang P, Harper JW, Elledge SJ, and Leder P (1995). Mice lacking p21CIP1/WAF1 undergo normal development, but are defective in G1 checkpoint control. *Cell* **82**, 675–684.

[20] Waldman T, Kinzler KW, and Vogelstein B (1995). p21 is necessary for the p53-mediated G1 arrest in human cancer cells. *Cancer Res* **55**, 5187–5190.

[21] Bunz F, Dutriaux A, Lengauer C, Waldman T, Zhou S, Brown JP, Sedivy JM, Kinzler KW, and Vogelstein B (1998). Requirement for p53 and p21 to sustain G2 arrest after DNA damage. *Science* **282**, 1497–1501.

[22] Dobin A, Davis CA, Schlesinger F, Drenkow J, Zaleski C, Jha S, Batut P, Chaisson M, and Gingeras TR (2013). STAR: ultrafast universal RNA-seq aligner. *Bioinformatics* **29**, 15–21.

[23] Li B and Dewey CN (2011). RSEM: accurate transcript quantification from RNA-Seq data with or without a reference genome. *BMC Bioinformatics* **12**, 323.

[24] Kanehisa M and Goto S (2000). KEGG: Kyoto encyclopedia of genes and genomes. *Nucleic Acids Res* **28**, 27–30.

[25] Subramanian A, Tamayo P, Mootha VK, Mukherjee S, Ebert BL, Gillette MA, Paulovich A, Pomeroy SL, Golub TR, and Lander ES, et al (2005). Gene set enrichment analysis: a knowledge-based approach for interpreting genome-wide expression profiles. *Proc Natl Acad Sci U S A* **102**, 15545–15550.

[26] Joshi-Tope G, Gillespie M, Vastrik I, D'Eustachio P, Schmidt E, de Bono B, Jassal B, Gopinath GR, Wu GR, and Matthews L, et al (2005). Reactome: a knowledgebase of biological pathways. *Nucleic Acids Res* **33**, D428–D432.

[27] Newman AM, Liu CL, Green MR, Gentles AJ, Feng W, Xu Y, Hoang CD, Diehn M, and Alizadeh AA (2015). Robust enumeration of cell subsets from tissue expression profiles. *Nat Methods* **12**, 453–457.

[28] Riley T, Sontag E, Chen P, and Levine A (2008). Transcriptional control of human p53-regulated genes. *Nat Rev Mol Cell Biol* **9**, 402–412.

[29] Allen MA, Andrysik Z, Dengler VL, Mellert HS, Guarnieri A, Freeman JA, Sullivan KD, Galbraith MD, Luo X, and Kraus WL, et al (2014). Global analysis of p53-regulated transcription identifies its direct targets and unexpected regulatory mechanisms. *Elife* **3**e02200.

[30] Kenzelmann Broz D, Spano Mello S, Bieging KT, Jiang D, Dusek RL, Brady CA, Sidow A, and Attardi LD (2013). Global genomic profiling reveals an extensive p53-regulated autophagy program contributing to key p53 responses. *Genes Dev* **27**, 1016–1031.

[31] Bunz F, Hwang PM, Torrance C, Waldman T, Zhang Y, Dillehay L, Williams J, Lengauer C, Kinzler KW, and Vogelstein B (1999). Disruption of p53 in human cancer cells alters the responses to therapeutic agents. *J Clin Invest* **104**, 263–269.

[32] Serrano M, Hannon GJ, and Beach D (1993). A new regulatory motif in cell-cycle control causing specific inhibition of cyclin D/CDK4. *Nature* **366**, 704–707.

[33] Alcorta DA, Xiong Y, Phelps D, Hannon G, Beach D, and Barrett JC (1996). Involvement of the cyclin-dependent kinase inhibitor p16 (INK4a) in replicative senescence of normal human fibroblasts. *Proc Natl Acad Sci U S A* **93**, 13742–13747.

[34] Sharpless NE and Sherr CJ (2015). Forging a signature of in vivo senescence. *Nat Rev Cancer* **15**, 397–408.

[35] Kurz DJ, Decary S, Hong Y, and Erusalimsky JD (2000). Senescence-associated (beta)-galactosidase reflects an increase in lysosomal mass during replicative ageing of human endothelial cells. *J Cell Sci* **113**(Pt 20), 3613–3622.

[36] Lee BY, Han JA, Im JS, Morrone A, Johung K, Goodwin EC, Kleijer WJ, DiMaio D, and Hwang ES (2006). Senescence-associated beta-galactosidase is lysosomal beta-galactosidase. *Aging Cell* **5**, 187–195.

[37] Coppe JP, Patil CK, Rodier F, Sun Y, Munoz DP, Goldstein J, Nelson PS, Desprez PY, and Campisi J (2008). Senescence-associated secretory phenotypes reveal cell-nonautonomous functions of oncogenic RAS and the p53 tumor suppressor. *PLoS Biol* **6**, 2853–2868.

[38] Rao SG and Jackson JG (2016). SASP: tumor suppressor or promoter? Yes! *Trends Cancer* **2**, 676–687.

[39] Mi H, Huang X, Muruganujan A, Tang H, Mills C, Kang D, and Thomas PD (2017). PANTHER version 11: expanded annotation data from Gene Ontology and Reactome pathways, and data analysis tool enhancements. *Nucleic Acids Res* **45**, D183–D189.

[40] Mi H, Muruganujan A, Casagrande JT, and Thomas PD (2013). Large-scale gene function analysis with the PANTHER classification system. *Nat Protoc* **8**, 1551–1566.

[41] Chien Y, Scuoppo C, Wang X, Fang X, Balgley B, Bolden JE, Premsrirut P, Luo W, Chicas A, and Lee CS, et al (2011). Control of the senescence-associated secretory phenotype by NF-kappaB promotes senescence and enhances chemosensitivity. *Genes Dev* **25**, 2125–2136.

[42] Wiley CD, Schaum N, Alimirah F, Lopez-Dominguez JA, Orjalo AV, Scott G, Desprez PY, Benz C, Davalos AR, and Campisi J (2018). Small-molecule MDM2 antagonists attenuate the senescence-associated secretory phenotype. *Sci Rep* **8**, 2410.

[43] Moreno CS, Matyunina L, Dickerson EB, Schubert N, Bowen NJ, Logani S, Benigno BB, and McDonald JF (2007). Evidence that p53-mediated cell-cycle-arrest inhibits chemotherapeutic treatment of ovarian carcinomas. *PLoS One* **2**e441.

[44] Roberson RS, Kussick SJ, Vallieres E, Chen SY, and Wu DY (2005). Escape from therapy-induced accelerated cellular senescence in p53-null lung cancer cells and in human lung cancers. *Cancer Res* **65**, 2795–2803.

[45] Sidi R, Pasello G, Opitz I, Soltermann A, Tutic M, Rehrauer H, Weder W, Stahel RA, and Felley-Bosco E (2011). Induction of senescence markers after neo-adjuvant chemotherapy of malignant pleural mesothelioma and association with clinical outcome: an exploratory analysis. *Eur J Cancer* **47**, 326–332.

[46] Wu PC, Wang Q, Grobman L, Chu E, and Wu DY (2012). Accelerated cellular senescence in solid tumor therapy. *Exp Oncol* **34**, 298–305.

[47] Wong KK, Izaguirre DI, Kwan SY, King ER, Deavers MT, Sood AK, Mok SC, and Gershenson DM (2013). Poor survival with wild-type TP53 ovarian cancer? *Gynecol Oncol* **130**, 565–569.

[48] Bataille F, Rummele P, Dietmaier W, Gaag D, Klebl F, Reichle A, Wild P, Hofstadter F, and Hartmann A (2003). Alterations in p53 predict response to preoperative high dose chemotherapy in patients with gastric cancer. *Mol Pathol* **56**, 286–292.

[49] Choi W, Porten S, Kim S, Willis D, Plimack ER, Hoffman-Censits J, Roth B, Cheng T, Tran M, and Lee IL, et al (2014). Identification of distinct Basal and luminal subtypes of muscle-invasive bladder cancer with different sensitivities to frontline chemotherapy. *Cancer Cell* **25**, 152–165.

[50] Tato-Costa J, Casimiro S, Pacheco T, Pires R, Fernandes A, Alho I, Pereira P, Costa P, Castelo HB, and Ferreira J, et al (2016). Therapy-induced cellular senescence induces epithelial-to-mesenchymal transition and increases invasiveness in rectal cancer. *Clin Colorectal Cancer* **15**, 170–178.e173.

[51] Rau B, Sturm I, Lage H, Berger S, Schneider U, Hauptmann S, Wust P, Riess H, Schlag PM, and Dorken B, et al (2003). Dynamic expression profile of p21WAF1/CIP1 and Ki-67 predicts survival in rectal carcinoma treated with preoperative radiochemotherapy. *J Clin Oncol* **21**, 3391–3401.

[52] Martin-Caballero J, Flores JM, Garcia-Palencia P, and Serrano M (2001). Tumor susceptibility of p21(Waf1/Cip1)-deficient mice. *Cancer Res* **61**, 6234–6238.